INVESTIGATION OF RAYLEIGH WAVE INTERACTION WITH SURFACE DEFECTS

Phan Hai Dang[a,*], Le Duc Tho[a], Le Quang Hung[b], Dao Duy Kien[c]

[a] *Institute of Theoretical and Applied Research, Duy Tan University, No 1 Phung Chi Kien street, Cau Giay district, Hanoi, Vietnam*
[b] *Graduate University of Science and Technology, VAST, 18 Hoang Quoc Viet street, Cau Giay district, Hanoi, Vietnam*
[c] *Faculty of Civil Engineering, HCMC University of Technology and Education, No 1 Vo Van Ngan street, Thu Duc district, Ho Chi Minh city, Vietnam*

Article history:
Received 08/08/2019, Revised 23/08/2019, Accepted 26/08/2019

Abstract

The current article is concerned with the interaction of Rayleigh waves with surface defects of arbitrary shape in a homogeneous, isotropic, linearly elastic half-space. Using a linear superposition principle, the interaction generates a scattered field which is equivalent to the field radiated from a distribution of horizontal and vertical tractions on the surface of the defect. These tractions are equal in magnitude but opposite in sign to the corresponding tractions obtained from the incident wave. The scattered field is then computed as the superposition of the displacements radiated from the tractions at every point of the defect surface using the reciprocity theorem approach. The far-field vertical displacements are compared with calculations obtained by the boundary element method (BEM) for circular, rectangular, triangular and arbitrary-shaped defects. Comparisons between the theoretical and BEM results, which are graphically displayed, are in excellent agreement. It is also discussed the limitations of the proposed approximate theory.

Keywords: half-space; Rayleigh wave; surface defect; reciprocity theorem; boundary element method (BEM).

https://doi.org/10.31814/stce.nuce2019-13(3)-09

1. Introduction

Surface waves, first investigated by [1], have been widely used in the area of nondestructive evaluation (NDE) for several decades. When engineering structures such as buildings, bridges, pipelines, ships and aircrafts contain surface defects not accessible for visual inspection, Rayleigh surface waves can be very useful in the detection and characterization of the defects. Understanding of Rayleigh interaction with surface defects is, therefore, critical to the further development of nondestructive evaluation techniques and material characterization methods.

Studies related to free surface waves propagating in half-spaces can be easily found in the textbooks [2–4] and the original articles, see for examples [1, 5]. Rayleigh wave motions subjected to surface or subsurface sources are very important for practical applications in science and engineering. They have also been largely investigated using the conventional integral transform method and the recent reciprocity approach [2, 6–16]. Scattering of Rayleigh waves by surface defects such as cracks, cavities and corrosion pits has been extensively considered in the literature. Typical examples

*Corresponding author. *E-mail address:* haidangphan.vn@gmail.com (Dang, P. H.)

of analytical work are the papers by [17–20]. Numerical work has been carried out by the finite element method [21–23], and the boundary element method [24, 25]. In a related category are papers on scattering by strips and grooves, see [20, 26–28]. Good agreement between numerical and experimental results of Rayleigh waves scattered by surface defects can be found in [4]. The approximate boundary conditions of shifting the loading of the defect on the flat surface was earlier explored by [29], see also Ogilvy's review article [30]. An approach based on matched asymptotic expansions was presented in [31].

In the current investigation, we propose a simple approach based on reciprocity theorems to investigate the scattering of Rayleigh waves from surface defects in a homogeneous elastic half-space. Compared to the previous results only for circular cavities obtained in [18], this work presents several calculations, results and discussions regarding different defects of circular, rectangular, triangular and arbitrary shapes. Comparisons between the theoretical computations and numerical results using boundary element method are graphically displayed and show excellent agreement. It is also discussed in this article the limitations of the proposed approach.

In the following, the paper is divided into four sections. Section 2 states the problem as the superposition of the incident wave and the scattered field. The scattered field, which is of interest in the current work, is equivalent to the field radiated by the tractions on the surface of defect. An analytical method based on reciprocity theorems to determine the displacement field of the surface waves radiated by a time-harmonic force is discussed in section 3. In section 4, detailed results and comparisons are presented followed by discussions on the limitations of the approximate approach. The conclusions are given in section 5.

2. Problem statement

Consider an isotropic elastic solid half-space $z \geq 0$ in Cartesian coordinate system, (x, y, z), which contains an arbitrary-shaped defect on the surface. A plane Rayleigh wave propagating in the x-direction is incident on the defect, see Fig. 1(a). Using the linear superposition technique, the total field $\mathbf{u}_{tot}$ may be written as

$$\mathbf{u}_{tot} = \mathbf{u}_{in} + \mathbf{u}_{sc} \tag{1}$$

where $\mathbf{u}_{in}$ is the incident field and the $\mathbf{u}_{sc}$ is scattered field.

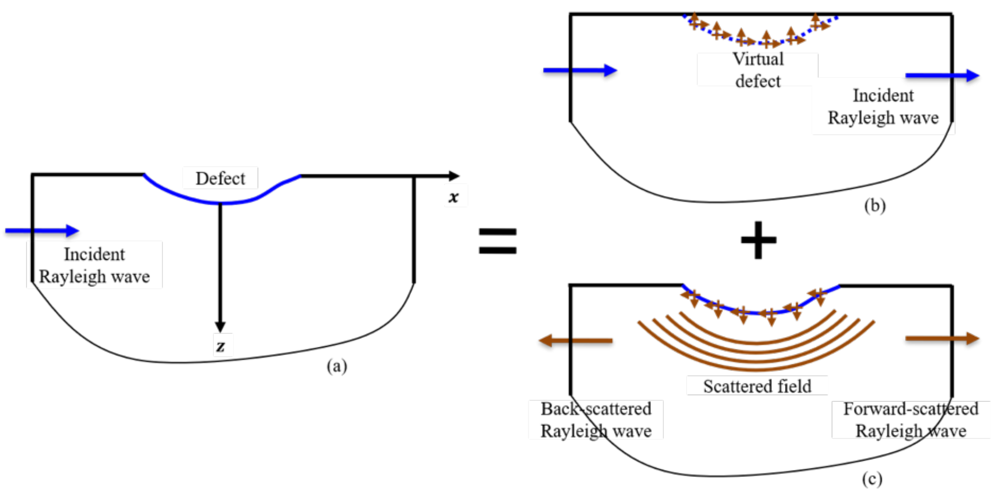

Figure 1. Linear superposition

By virtue of linear superposition shown in Fig. 1, the scattered field is equivalent to the field generated by the application of a distribution of tractions applied on the surface of the defect. These tractions can be calculated from the corresponding tractions due to the incident wave on a virtual defect in the half-space without defect. The horizontal and vertical tractions can therefore be calculated from the stress components of the incident Rayleigh wave and the outward normal vectors of the defect surface. The tractions, in turn, generate a radiated field which is equivalent to the scattered wave field. It is noted that the tractions on the surface of the defect generate body waves as well as surface waves. The surface waves, which do not suffer geometrical attenuation, dominate at sufficiently large values of $|x|$.

The traction components are first calculated for every point of the defect surface. The reciprocity theorem is then applied to the equivalent time-harmonic loads that are applied on the surface of the half-space, to obtain the displacement amplitudes of the scattered field. The total displacement amplitude is a superposition of the amplitudes generated by the horizontal and vertical loads at every point on the surface.

3. Rayleigh waves generated by a distribution of loadings

The surface waves considered in this research are two-dimensional and nondispersive. In addition to that its amplitude decreases with depth, a surface wave is defined by the angular frequency ω, the wavenumber k, where $k = \dfrac{\omega}{c}$ with c being the surface wave velocity, the Lame constants λ, μ and the mass density ρ. The displacements may be written as [18]

$$u_x = \pm iAU(z)\, e^{\pm ikx}, \quad u_z = AW(z)\, e^{\pm ikx} \tag{2}$$

where the time-harmonic term $\exp(i\omega t)$ has been omitted for simplicity, and the plus and minus signs apply to Rayleigh waves traveling in the negative and positive x-direction, respectively. In Eq. (2)

$$U(z) = d_1 e^{-kpz} + d_2 e^{-kqz}, \quad W(z) = d_3 e^{-kpz} - e^{-kqz} \tag{3}$$

where

$$p = \sqrt{1 - \frac{c^2}{c_L^2}}, \quad q = \sqrt{1 - \frac{c^2}{c_T^2}} \tag{4}$$

with

$$c_L = \sqrt{\frac{\lambda + 2\mu}{\rho}}, \quad c_T = \sqrt{\frac{\mu}{\rho}} \tag{5}$$

which are the longitudinal and transverse wave velocities, respectively. Dimensionless d_1, d_2, d_3 are defined by

$$d_1 = \frac{-\left(1 + q^2\right)}{2p}, \quad d_2 = q, \quad d_3 = \frac{1 + q^2}{2} \tag{6}$$

The corresponding stresses can be easily calculated using Hooke's law

$$\tau_{xx} = AT_{xx}(z)\, e^{\pm ikx}, \quad \tau_{xz} = \pm iAT_{xz}(z)\, e^{\pm ikx}, \quad \tau_{zz} = AT_{zz}(z)\, e^{\pm ikx} \tag{7}$$

where

$$T_{xx}(z) = k\mu\left(d_4 e^{-kpz} + d_5 e^{-kqz}\right) \tag{8}$$

$$T_{xz}(z) = k\mu\left(d_6 e^{-kpz} + d_7 e^{-kqz}\right) \tag{9}$$

$$T_{zz}(z) = k\mu\left(d_8 e^{-kpz} + d_9 e^{-kqz}\right) \tag{10}$$

with

$$d_4 = \frac{\left(1+q^2\right)\left(1+2p^2-q^2\right)}{2p}, \quad d_5 = -2q, \quad d_6 = -d_7 = 1+q^2, \quad -d_8 = d_9 = 2q \tag{11}$$

Reciprocity theorems in general offer a relation between displacements, tractions and body forces of two different loading states of an elastic body as given in the following equation (see References [6, 9])

$$\int_V \left(f_j^A u_j^B - f_j^B u_j^A\right) dV = \int_S \left(\tau_{ij}^B u_j^A - \tau_{ij}^A u_j^B\right) n_i dS, \quad i, j = x, z \tag{12}$$

where S is the contour around the domain V, f_j indicates the body forces, n_i is the components of the unit vector along the outward normal to S, and A, B denotes two elastodynamic states. These relations were used to obtain surface wave motions in a half-space, see for examples [6, 8, 9, 17]. In this section, they are applied to solve the scattering of surface waves by a surface defect.

The approximate approach to the analysis of surface waves scattered by a defect at the surface of an elastic half-space is applied to a defect that has an arbitrary shape. Suppose that the defect shape is defined as $z = h(x)$. For the problem given in Fig. 1(c), the tractions are the horizontal and vertical surface forces which need to be calculated. The forces on the virtual defect boundary at (x_0, z_0) are

$$f_x(x_0, z_0) = \tau_{xx}(x_0, z_0)\, h'(x_0)\, dx_0 - \tau_{xz}(x_0, z_0)\, dx_0 \tag{13}$$

$$f_z(x_0, z_0) = \tau_{xz}(x_0, z_0)\, h'(x_0)\, dx_0 - \tau_{zz}(x_0, z_0)\, dx_0 \tag{14}$$

Using the expressions of displacement and stress components of the incident field yields

$$f_x(x_0, z_0) = -A_{in}\left[T_{xx}(z_0)\, h'(x_0) + iT_{xz}(z_0)\right] e^{-ikx_0} dx_0 \tag{15}$$

$$f_z(x_0, z_0) = -A_{in}\left[iT_{xz}(z_0)\, h'(x_0) + T_{zz}(z_0)\right] e^{-ikx_0} dx_0 \tag{16}$$

where A_{in} is the amplitude of the incident wave and $z_0 = h(x_0)$. These loads will generate surface waves in both positive and negative directions. The reciprocity theorems are then used to obtain the displacements of the scattered field. The detailed computation is introduced in [6, 18]. Note that the radiation from the opposites in sign of the distributions with respect to x_0 of these surface forces approximates the scattering of an incident surface wave by the defect. The forward radiation $(x > 0)$ and the backward radiation $(x < 0)$ are, respectively,

$$u_z^{A+}(x, z) = \frac{iA^+(x_0, z_0)}{2I} F^+(x_0, z_0)\, dx_0 W^R(z)\, e^{-ikx} \tag{17}$$

$$u_z^{A-}(x, z) = \frac{iA^-(x_0, z_0)}{2I} F^-(x_0, z_0)\, e^{-2ikx_0} dx_0 W^R(z)\, e^{ikx} \tag{18}$$

where

$$F^+(x_0, z_0) = i\left[T_{xx}(z_0)\, h'(x_0) + iT_{xz}(z_0)\right] U(0) - \left[iT_{xz}(z_0)\, h'(x_0) + T_{zz}(z_0)\right] W(0) \tag{19}$$

$$F^-(x_0, z_0) = -i\left[T_{xx}(z_0)\, h'(x_0) + iT_{xz}(z_0)\right] U(0) - \left[iT_{xz}(z_0)\, h'(x_0) + T_{zz}(z_0)\right] W(0) \tag{20}$$

Eqs. (19) and (20) represent the radiation from individual surface forces located at $x = x_0$. To obtain the radiation of the distributions of surface forces, we integrate these equations over x_0 from $x_0 = x_1$ to $x_0 = x_2$. For the displacements on the surface ($z = 0$), we may write

$$u_z^{A+} = A_{sc}^{+} W(0)\, e^{-ikx} \tag{21}$$

$$u_z^{A-} = A_{sc}^{-} W(0)\, e^{ikx} \tag{22}$$

where

$$\frac{A_{sc}^{+}}{A_{in}} = \frac{i}{2I}\int_{x_1}^{x_2} F^{+}(x_0, z_0)\, dx_0 \tag{23}$$

$$\frac{A_{sc}^{-}}{A_{in}} = \frac{i}{2I}\int_{x_1}^{x_2} F^{-}(x_0, z_0)\, e^{-2ikx_0} dx_0 \tag{24}$$

are amplitude ratios between the scattered field and incident field. Note that the integrals appearing in Eqs. (23) and (24) may be analytically obtained for defects of well-defined shape. In general, however, a numerical procedure should be used to compute the amplitude ratios.

4. Results and discussions

In this section, the absolute values of the amplitude ratios given in Eqs. (23) and (24) are plotted for different defect shapes in comparison with numerical results by the boundary element method. We have built a BEM code using Fortran taking into account the idea of Rayleigh wave correction presented in Ref. [24]. This idea is simple that allows the Rayleigh waves propagating along the free surface of the half-space to escape the computational domain without producing spurious reflections from its limits. In our computer program, the boundary conditions applying for the scattered field are the traction values obtained theoretically at the positions of the defect boundary but of the opposite sign.

Note that theoretical results obtained by the proposed approach can conveniently and proficiently provide understanding of generation, propagation, reflection, transmission, and scattering of ultrasound which is essential to build measurement models for quantitative ultrasonic methods. They also allow us to perform and adjust ultrasonic tests on an interactive basis, thus providing us with an effective response process to improve data acquisition and gaining more information about the characteristics of the defects. However, this approach is an approximation and should have certain limitations. Therefore, the BEM results, which are assumed to be close to the exact solutions, are used to examine the accuracy of the approximation.

The geometry of the defects, which are characterized by the depth D and half of the width R_0, is shown in Figs. 2(a), (b), (c) and (d). The comparisons are plotted versus the dimensionless quantities kR_0. In all cases of study, the material is chosen as steel having a shear modulus of $\mu = 7.9872 10^{10}\ \dfrac{\mathrm{N}}{\mathrm{m}^2}$, a Lame's constant of $\lambda = 11.031 10^{10}\ \dfrac{\mathrm{N}}{\mathrm{m}^2}$, and a density of $\rho = 7800\ \dfrac{\mathrm{kg}}{\mathrm{m}^2}$. In the following representation of the results, we fix $D = 0.1$ mm and $R_0 = 1.0$ mm and vary the frequency from $f = 0.1$ MHz to $f = 1.0$ MHz so that kR_0 also varies. The values of $\left|\dfrac{A_{sc}^{-}}{A_{in}}\right|$ and $\left|\dfrac{A_{sc}^{-}}{A_{in}}\right|$ are thus dependent only on the dimensionless quantities kR_0.

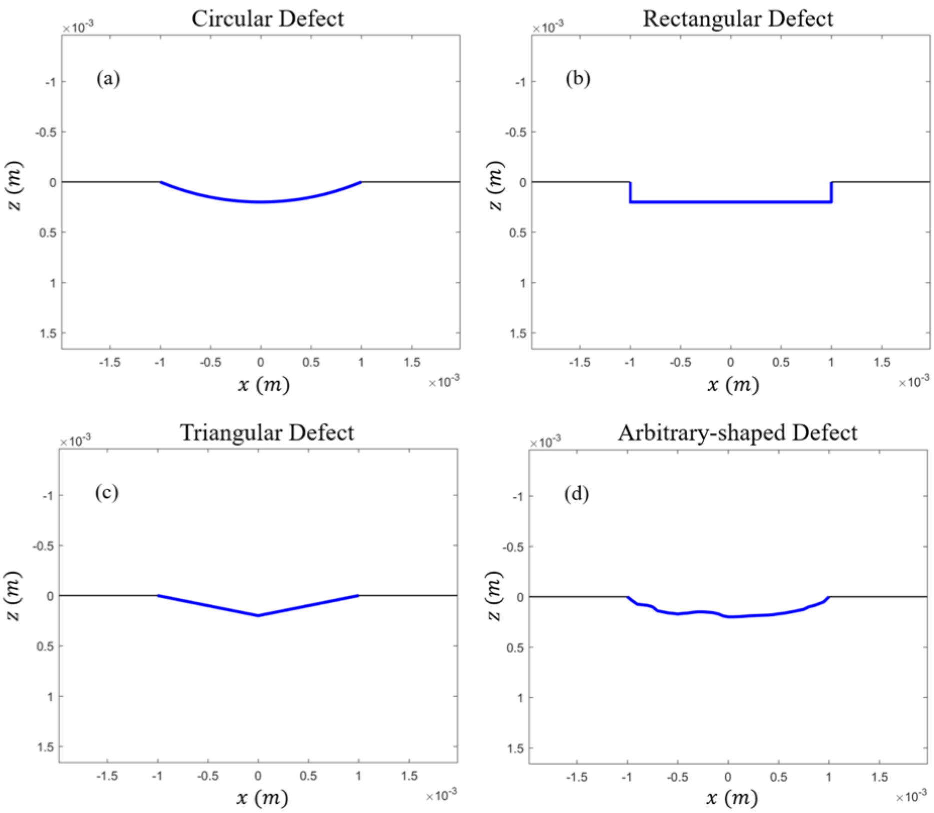

Figure 2. Defect geometry

Four cases of study are for circular, rectangular, triangular and general arbitrary-shaped defects (Fig. 2). Absolute values of the amplitude ratios regarding scattering of surface waves by a circular defect are shown in Fig. 3. In general, the comparisons between are in excellent agreement. As $kR_0 \geq 1.5$, a slight difference between the analytical and the BEM results appears for the backscattering. This is due to for the existence of the term $e^{-2i\bar{x}_0}$, where $\bar{x}_0 = kx_0$ in Eq. (23).

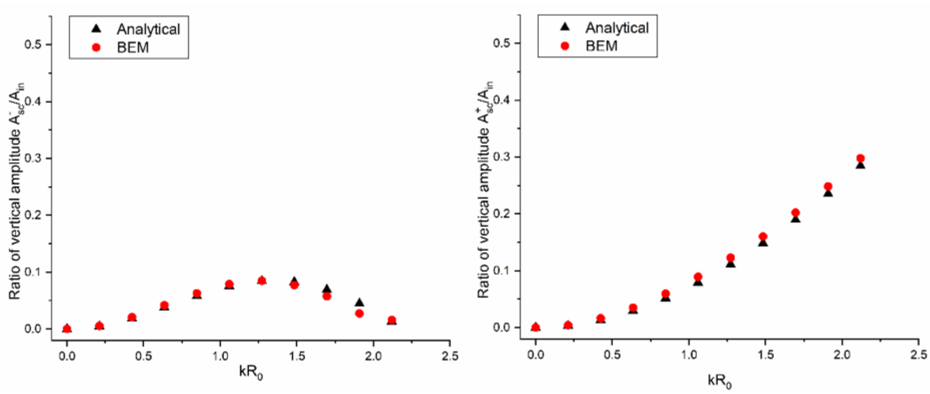

Figure 3. Backscattering (left) and forward scattering (right) of a circular defect:
$R_0 = 1.0$ mm, $D = 0.1$ mm, 0.1 MHz $\leq f \leq$ 1.0 MHz

The comparisons for rectangular and triangular defects are presented in Figs. 4 and 5, respectively. In the case of a rectangular defect, the comparison is in good agreement as $kR_0 \leq 1$, especially for the forward scattering and shows a clear difference when $kR_0 \geq 1$. This shows the limitations of the proposed approach to the defect having sharp surface. Meanwhile, the comparisons between the analytical and the BEM calculations show excellent agreement for the case of a triangular defect.

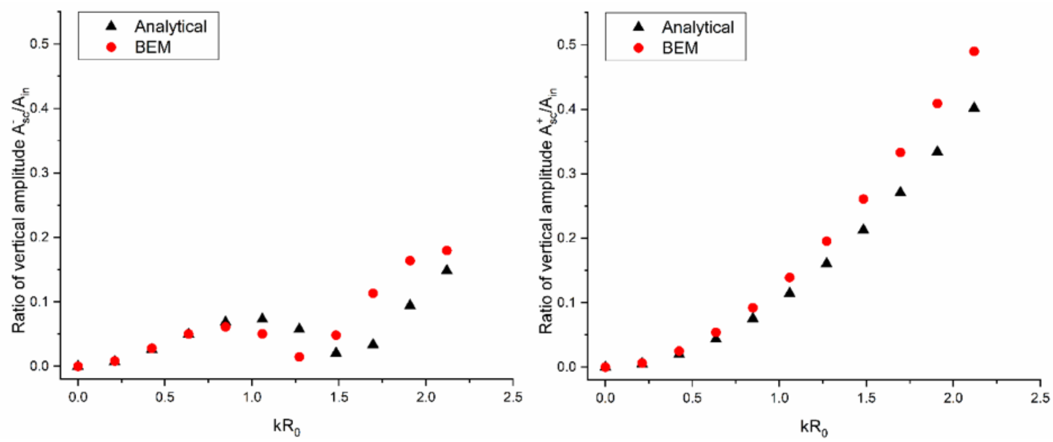

Figure 4. Backscattering (left) and forward scattering (right) of a rectangular defect: $R_0 = 1.0$ mm, $D = 0.1$ mm, 0.1 MHz $\leq f \leq$ 1.0 MHz

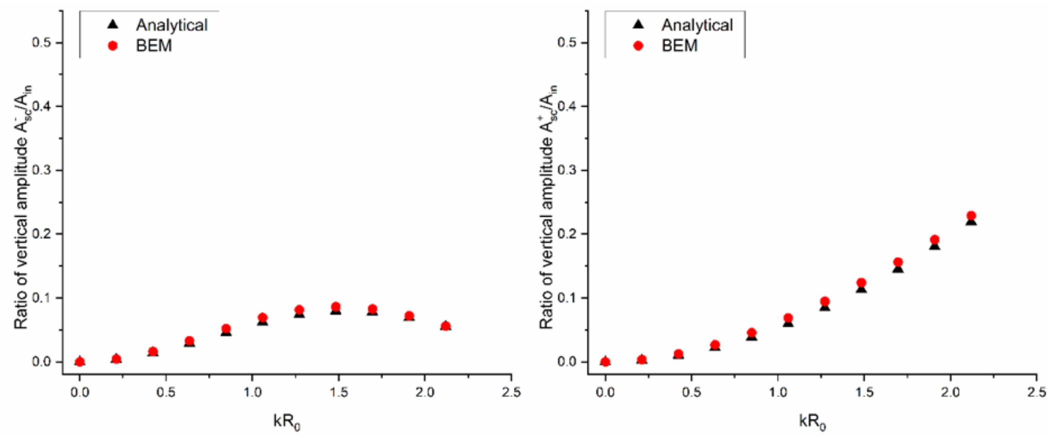

Figure 5. Backscattering (left) and forward scattering (right) of a triangular defect: $R_0 = 1.0$ mm, $D = 0.1$ mm, 0.1 MHz $\leq f \leq$ 1.0 MHz

The amplitude ratios corresponding to scattering of surface waves by a defect of arbitrary shape are shown in Fig. 6. Note that the depth of the defect is calculated from the lowest point of the defect to the surface of the half-space. The volume of this defect is chosen to be similar to the one of circular defect, but their shapes are different. The comparisons are also in very good agreement as in the case of the circular one. The backscattering amplitude ratios in the two cases behave similarly as $kR_0 \leq 1.5$ and start to have slightly different as $kR_0 \geq 1.5$.

It can also be seen in Figs. 3 to 6 that for the forward scattering, the largest amplitude ratios come from the rectangular defect while the smallest ones are of the triangular defect. This can be explained that the volume of defect or defect size is another critical parameter to scattering phenomenon.

In summary, the comparisons between the analytical and BEM results from Figs. 3 to 6 show not only excellent agreement but also slight differences for different defects. The analytical approach presented in this paper has the limitations. Excellent agreement is shown for small parameter kR_0 and

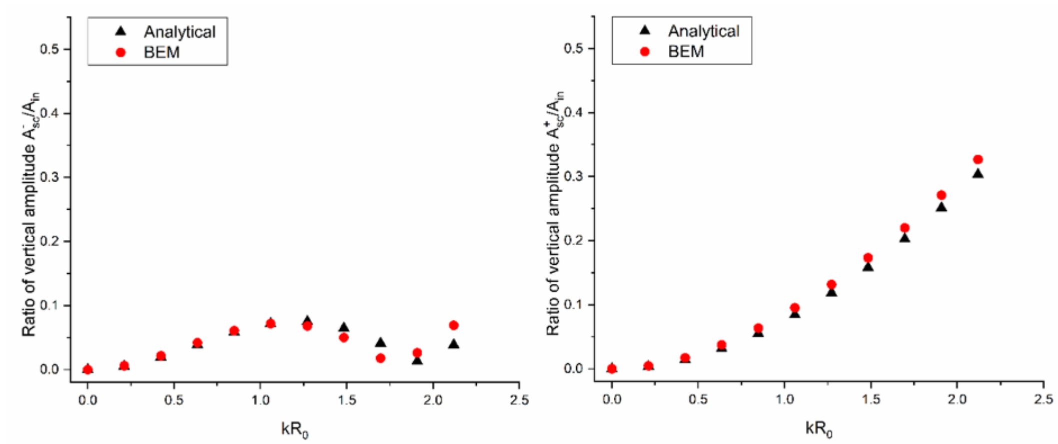

Figure 6. Backscattering (left) and forward scattering (right) of an arbitrary-shaped defect: $R_0 = 1.0$ mm, $D = 0.1$ mm, 0.1 MHz $\leq f \leq$ 1.0 MHz

small volume of the defect. The difference increases with the increase of dimensionless quantity kR_0. It can be explained as that as kR_0 rises and kD is fixed, the volume of the defect increases. For the case of the backscattering, the existence of the term $e^{-2i\bar{x}_0}$ appearing in Eq. (23) also affects the accuracy of the proposed approximation.

5. Conclusions

It has been shown in this article that the scattering of surface waves by a two-dimensional defect of arbitrary shape in an elastic half-space can be solved in a simple manner by application of the elastodynamic reciprocity theorems. We have theoretically derived the ratios of the vertical displacement amplitudes of the scattered surface waves to those of the incident surface waves in terms of dimensionless quantities. The comparisons with BEM results have shown the validation of the analytical approximation for certain ranges of the parameters kR_0 and the volume of defect. It can be seen in this investigation that the proposed theoretical approach has given a quite good agreement for the rectangular defect, and excellent agreement for the circular, triangular and arbitrary-shaped defects.

Acknowledgement

This research is funded by Vietnam National Foundation for Science and Technology Development (NAFOSTED) under grant number 107.02-2019.21.

References

[1] Rayleigh, L. (1885). On waves propagated along the plane surface of an elastic solid. *Proceedings of the London Mathematical Society*, 1(1):4–11.
[2] Achenbach, J. (2012). *Wave propagation in elastic solids*, volume 16. Elsevier.
[3] Rose, J. L. (2014). *Ultrasonic guided waves in solid media*. Cambridge University Press.
[4] Viktrov, I. A. (1970). *Rayleigh and Lamb waves: physical theory and applications*. Plenum Press.
[5] Lamb, H. (1904). On the propagation of tremors over the surface of an elastic solid. *Philosophical Transactions of the Royal Society of London, Series A*, 203:1–42.
[6] Phan, H., Cho, Y., Achenbach, J. D. (2013). Validity of the reciprocity approach for determination of surface wave motion. *Ultrasonics*, 53(3):665–671.

[7] Phan, H., Cho, Y., Achenbach, J. D. (2014). Verification of surface wave solutions obtained by the reciprocity theorem. *Ultrasonics*, 54(7):1891–1894.

[8] Phan, H., Cho, Y., Le, Q. H., Pham, C. V., Nguyen, H. T.-L., Nguyen, P. T., Bui, T. Q. (2019). A closed-form solution to propagation of guided waves in a layered half-space under a time-harmonic load: An application of elastodynamic reciprocity. *Ultrasonics*, 96:40–47.

[9] Achenbach, J. D. (2003). *Reciprocity in elastodynamics*. Cambridge University Press.

[10] Ewing, W. M., Zardetzky, W. S., Press, F. (1957). *Elastic waves in layered media*. McGraw-Hill.

[11] Pekeris, C. L. (1955). The seismic surface pulse. *Proceedings of the National Academy of Sciences of the United States of America*, 41(7):469–480.

[12] Pinney, E. (1954). Surface motion due to a point source in a semi-infinite elastic medium. *Bulletin of the Seismological Society of America*, 44(4):571–596.

[13] Phan, H., Cho, Y., Pham, C. V., Nguyen, H., Bui, T. Q. (2019). A theoretical approach for guided waves in layered structures. In *AIP Conference Proceedings*, volume 2102, AIP Publishing, page 050011.

[14] Phan, H., Bui, T. Q., Nguyen, H. T.-L., Pham, C. V. (2018). Computation of interface wave motions by reciprocity considerations. *Wave Motion*, 79:10–22.

[15] Nguyen, P.-T., Phan, H. (2019). A theoretical study on propagation of guided waves in a fluid layer overlying a solid half-space. *Vietnam Journal of Mechanics*, 41(1):51–62.

[16] Phan, H., Cho, Y., Ju, T., Achenbach, J. D. (2014). Multiple scattering of surface waves by cavities in a half-space. In *AIP Conference Proceedings*, volume 1581, AIP, 537–541.

[17] Auld, B. A. (1979). General electromechanical reciprocity relations applied to the calculation of elastic wave scattering coefficients. *Wave Motion*, 1(1):3–10.

[18] Phan, H., Cho, Y., Achenbach, J. D. (2013). Application of the reciprocity theorem to scattering of surface waves by a cavity. *International Journal of Solids and Structures*, 50(24):4080–4088.

[19] Phan, H., Cho, Y., Li, W. (2018). A theoretical approach to multiple scattering of surface waves by shallow cavities in a half-space. *Ultrasonics*, 88:16–25.

[20] Gregory, R. D., Austin, D. M. (1990). Scattering of waves by a semicylindrical groove in the surface of an elastic half-space. *The Quarterly Journal of Mechanics and Applied Mathematics*, 43(3):293–315.

[21] Hassan, W., Veronesi, W. (2003). Finite element analysis of Rayleigh wave interaction with finite-size, surface-breaking cracks. *Ultrasonics*, 41(1):41–52.

[22] Yuan, M., Zhang, J., Song, S.-J., Kim, H.-J. (2015). Numerical simulation of Rayleigh wave interaction with surface closed cracks under external pressure. *Wave Motion*, 57:143–153.

[23] Khuong, L. N. (2017). Modelling of CFRP strengthening on the behavior of RC slender columns. *Journal of Science and Technology in Civil Engineering (STCE)-NUCE*, 11:70–76.

[24] Arias, I., Achenbach, J. D. (2004). Rayleigh wave correction for the BEM analysis of two-dimensional elastodynamic problems in a half-space. *International Journal for Numerical Methods in Engineering*, 60(13):2131–2146.

[25] Liu, W., Cho, Y., Phan, H., Achenbach, J. D. (2011). Study on the scattering of 2-D Rayleigh waves by a cavity based on BEM simulation. *Journal of Mechanical Science and Technology*, 25(3):797–802.

[26] Kosachev, V. V., Lokhov, Y. N., Chukov, V. N. (1990). On the theory of scattering the Rayleigh surface acoustic waves by a two-dimensional statistical roughness of a free solid surface. *Solid State Communications*, 73(8):535–539.

[27] Simons, D. A. (1978). Reflection of Rayleigh waves by strips, grooves, and periodic arrays of strips or grooves. *The Journal of the Acoustical Society of America*, 63(5):1292–1301.

[28] Tuan, H.-S., Li, R. C. M. (1974). Rayleigh-wave reflection from groove and step discontinuities. *The Journal of the Acoustical Society of America*, 55(6):1212–1217.

[29] Gilbert, F., Knopoff, L. (1960). Seismic scattering from topographic irregularities. *Journal of Geophysical Research*, 65(10):3437–3444.

[30] Ogilvy, J. A. (1987). Wave scattering from rough surfaces. *Reports on Progress in Physics*, 50(12):1553.

[31] Abrahams, I. D., Wickham, G. R. (1992). Scattering of elastic waves by an arbitrary small imperfection in the surface of a half-space. *Journal of the Mechanics and Physics of Solids*, 40(8):1683–1706.